Data Collection Techniques for Preradioimmunotherapy Imaging

Lawrence D. Durack and Janet F. Eary

Department of Radiology, Division of Nuclear Medicine, University of Washington Medical Center, Seattle, Washington

Objective: Estimation of absorbed radiation doses to normal organs is essential for use of radiolabeled monoclonal antibodies in cancer therapy. We have developed methods for acquiring gamma camera images that provide precise and reproducible biodistribution data for dosimetry calculations.
Methods: Patient attenuation data is acquired by imaging a radioactive sheet source both with and without the patient between the source and the camera. Organ localization is performed by identifying landmarks on the patient and then injecting ^{99m}Tc agents that visualize the major organs. Using templates placed over the camera positioning scope and point source markers on anatomic landmarks, the patient is positioned for each view and the templates are marked where the sources appear. After radiolabeled antibody infusion the patient is positioned using point source markers and the previously created templates.
Results: We have developed a systematic method which has reduced the amount of time needed for biodistribution data acquisition and processing.
Conclusion: This precise method gives the investigator confidence when comparing pretreatment radiation absorbed dose estimates to the patient post-treatment outcome.
Key Words: monoclonal antibodies; biodistribution; cancer therapy

J Nucl Med Technol 1995; 23:65–69

Monoclonal antibody imaging trials for cancer localization are being performed at many institutions (*1–9*). When tumor localization is consistently high and the institution has facilities to do so, radioimmunotherapy is considered (*1,2,7,9–21*).

At our institution we evaluate patients with B-cell non-Hodgkin's lymphoma and acute leukemia for possible radioimmunotherapy (*10,11,13,14,19–21*). Multiple trace-labeled antibody infusions at increasing concentrations are performed on each patient to determine antibody residence times for each organ and whole body. If a patient shows favorable tumor-to-normal tissue accumulation of the antibody, that patient is treated with a single dose of antibody labeled with a high-level of ^{131}I. It is therefore necessary to have an imaging method that produces consistently accurate organ uptake and clearance data. In this developmental work, the method must also eliminate intra-observer variation. The ability to compare data from two or three infusions on the same patient, as well as between similar studies performed on different patients, is required for our protocols. Prior to antibody infusion, all patients are prepared in such a way that postinfusion data is reproducible and accurate.

For reprints and correspondence contact: Lawrence Durack, University Medical Center, Division of Nuclear Medicine RC-70, 1956 NE Pacific, Seattle, WA 98195.

STUDY OUTLINE

Patients selected for this protocol have disease that is resistant to conventional chemotherapy. Tumor samples in lymphoma, or bone marrow samples in leukemia, must be shown to react with available antibodies before beginning the protocol. Other major organs must be functioning normally and the candidates may not have had systemic chemotherapy in the month prior to study. Also, the patient's disease must be progressing slowly enough that several trace-labeled studies can be performed without jeopardizing the patient's chances for a favorable outcome, if the patient proceeds to treatment.

All patients receive an antibody dose based on their body weight. The antibody is labeled by the chloramine T method (*22*) with 5–10 mCi of ^{131}I. Biodistribution of the labeled antibody is followed by gamma camera imaging immediately following infusion and, in the case of leukemia patients, at 4, 18, 24, 48 and 72 hr postinfusion. For patients with lymphoma, images are acquired immediately and at 24, 48, 120 and 148 hr postinfusion. Radioiodine content in normal organs is determined from opposing view gamma camera images for each timepoint (*13,23–27*). Time-activity curves for antibody in marrow are created from multiple regions of interest drawn over known sites of viable marrow. Tumor uptake and clearance curves in lymphoma are derived from regions of interest drawn over image-positive tumor sites in the groins and axillae. Serum clearance and urinary excretion curves are plotted using data from serial blood samples and urine collections. Quantitative uptake is determined by comparison to an aliquot of the injectate.

MATERIALS AND METHODS

The MIRD model (*28–30*) is used to calculate the absorbed dose to organs and tumors. Since MIRD models were designed to estimate doses to normal organs only, tumors are assigned locations and masses corresponding to normal organs of similar size and location for determining their cross-organ doses. Also, it is assumed that isotope deposition in organs and tumors is uniform. "Standard man" organ volumes in the MIRD model are adjusted to those calculated from whole-body CT scans performed on each patient (*31*).

Estimation of absorbed dose to an organ is derived from the area under the time-activity curve for that organ (mCi-hr/g) multiplied by the physical constant for the isotope used (g-rads/mCi-hr). This is the integrated area under the time-activity curves derived from serial gamma camera images multiplied by the S factor for ^{131}I. Since the S factor for ^{131}I is known, what remains is to accurately quantitate the ^{131}I content in every organ at each timepoint.

The formula for quantitative uptake in a site using the opposing view method (*23,26*) determines the data that must be gathered for each site:

$$A = (I_a I_p)^{1/2} e^{(\mu e T/2)} f/c, \qquad \text{Eq. 1}$$

where A = activity in the organ (μCi), I_a = anterior counts (cpm), I_p = posterior counts (cpm), μe = coefficient of attenuation (cm^{-1}), T = patient thickness (cm), f = self attenuation coefficient (cm^{-1}), and c = system calibration factor (cpm/μCi).

The calculation $e^{(\mu e T/2)} f$ represents an estimate of attenuation of each body region, and is replaced by a direct measurement of patient attenuation. Attenuation in the chest and abdomen are different because of variable tissue density. For example, the lung volumes are largely air, yielding a markedly different attenuation correction than in the abdomen over the liver. To accomplish regional attenuation measurement, a fluid-filled sheet source is loaded with approximately 5 mCi ^{131}I and gently agitated until the isotope is evenly distributed. It is then placed beneath the scanning table directly under the camera (Fig. 1). A five-minute image is acquired of the source alone, with one patient thickness between the camera and imaging table. Without moving the source, a five-minute image is acquired of the chest. Similarly, a five-minute image of the abdomen is performed. With these data, $e^{(\mu e T/2)} f$ in the formula can be replaced by:

$$1/\sqrt{(I_t/I_O)}, \qquad \text{Eq. 2}$$

where I_t is the counts in a region of the patient transmission image, and I_O is the counts in the same region of the field flood image.

Following the attenuation measurement a blood volume determination is made using a commercially available kit of HSA labeled with ^{125}I. This is done to accurately compare the volume of distribution of the antibody to plasma volume. An accurate plasma volume is an important factor in calculating the volume of antibody distribution and understanding the kinetics of antibody transport because antibodies leave the circulation at varying rates and often distribute rapidly into the total body water. The blood volume determination also allows us to perform dosimetry evaluations of tissues not imaged by the gamma camera.

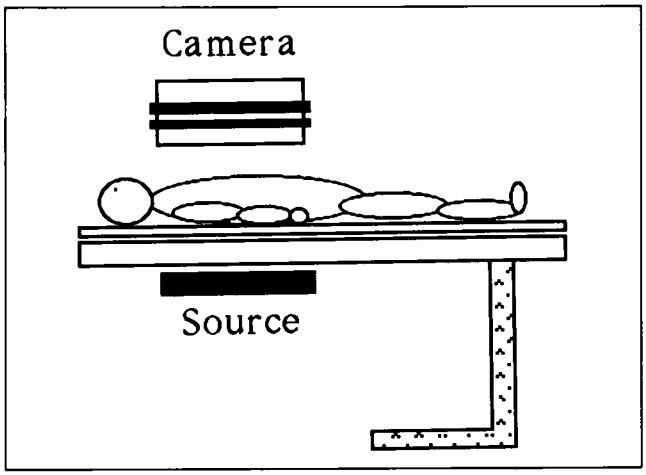

FIGURE 1. Patient, camera and sheet source in position to acquire an attenuation image.

Resolution of normal organs with ^{131}I is often poor, particularly at late timepoints after antibody infusion when count rates are low. To facilitate creation of accurate normal organ region of interest outlines, we image the lungs, liver and spleen, and kidneys with ^{99m}Tc-labeled agents, taking advantage of the superior image resolution of ^{99m}Tc.

Use of the same regions at each timepoint necessitates accurate repositioning of the patient on serial imaging days. Preparation for organ imaging is begun by making transparent film templates which are cut to a size that can be conveniently placed over the camera positioning scope. These templates are marked on their corners or borders so they can be oriented correctly on the scope each time they are used. Two markers are made of ^{99m}Tc-soaked cotton-tipped applicators inside needle shields. Anatomic landmarks are placed on the patient's skin using an indelible marking pen. Anterior landmarks are the suprasternal notch, xyphoid and umbilicus. Posteriorly the spine is marked at C-7, near the diaphragm and just above the belt line.

Organ imaging is begun by injecting the patient with ~4 mCi ^{99m}Tc MAA for lung visualization. After placing the spot markers for the suprasternal notch and xyphoid, the patient is positioned under the camera with both lungs in the field of view (Fig. 2). The film template for the anterior chest is taped into place on the positioning scope. The locations of the radioactive markers on the patient are marked on the film template. The ^{99m}Tc markers are then removed from the field of view without moving the patient and an image is acquired. This, and all other technetium images, is acquired for one million counts. The film template is labeled ANT CHEST and marked with the patient's name or other identifier, and set aside for later use. For a posterior lung image, the patient lies on his stomach and the ^{99m}Tc markers are placed on the C-7 and diaphragm landmarks. The patient is

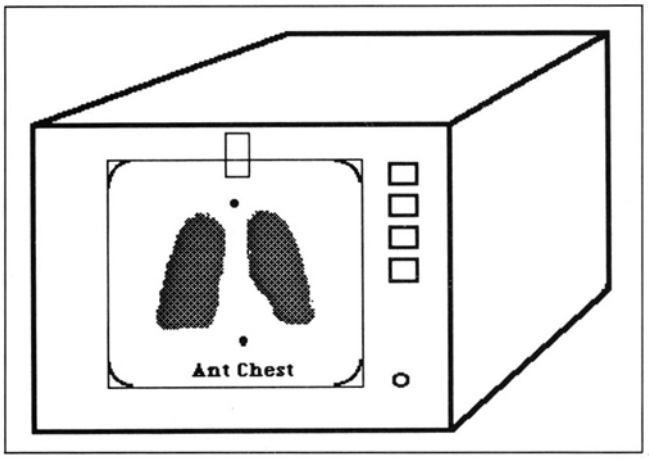

FIGURE 2. Image of patient's lungs on positioning scope with template for the anterior chest overlaid.

aligned under the camera and a template for the posterior chest is placed over the positioning scope. The locations of the markers on the patient's back are recorded on the film template with a permanent marker, the template is labeled POST CHEST. The radioactive markers are removed and an image is acquired.

The patient is then injected with 20 mCi ^{99m}Tc glucoheptonate to visualize the kidneys. With the patient lying on his back, ^{99m}Tc spot markers are placed on the xyphoid and umbilicus. The patient is positioned with kidneys in the lower half of the field and the lung bases visible in the upper part of the field. We have a camera with a 400-mm diameter field of view, therefore extra care is taken with this aspect of the positioning since the entire liver and spleen must also appear in the images of the abdomen. After determining that the patient is correctly positioned, another film template is affixed to the persistence scope, marked, and labeled ANT ABD. The ^{99m}Tc markers are removed and another image is acquired. With the patient lying on his stomach, the spot markers are placed on the diaphragm and belt line marks, and the patient is positioned under the camera as with the anterior abdomen image previously described. Once again, a new template is affixed, labeled, identified as POST ABD and marked for later use. An image is acquired of the posterior abdomen.

The patient is then injected with 5 mCi ^{99m}Tc sulfur colloid for liver imaging and, after 10 min, positioned on his back under the camera with spot markers on the xyphoid and umbilicus. The ANT ABD template is replaced over the positioning scope exactly as it was initially. The patient is then positioned by lining up the marks on the template with the ^{99m}Tc markers on the patient. The anatomic markers are removed and another image is recorded. Finally, with the patient on his stomach and the spot markers on the spine at the diaphragm and belt line, the POST ABD template is affixed to the scope, the patient is aligned with the marks on the template overlying the anatomic markers. The ^{99m}Tc markers are then removed and the liver/spleen localization image is acquired. By following this sequence of ^{99m}Tc imaging, the technologist can later draw more precise organ regions, thereby reducing the chance for errors in subsequent ^{131}I organ content determinations.

Prior to ^{131}I-labeled antibody infusion a camera and uptake probe standard must be created. For both gamma camera imaging and whole-body counting, a standard must be counted at each timepoint to correct for isotope decay and electronic drift. One mCi ^{131}I is placed in a 250-cc tissue culture flask filled with water. The exact ^{131}I amount and time of calibration are recorded.

ANTIBODY BIODISTRIBUTION STUDIES

After ^{131}I-labeled antibody infusion, gamma camera images are acquired immediately. Using the previously created standard, a full-width half-maximum window is set around the primary photopeak of ^{131}I (364 keV). For our system this is approximately a 13% window. On subsequent days, for each image of the chest and abdomen, the appropriate template is placed on the camera persistence scope and the patient is positioned under the camera using ^{99m}Tc markers placed on anatomic skin marks. The patient is positioned so that the markers are aligned with the marks on the respective template. Patients are imaged at the timepoints mentioned earlier, and the same method of realignment using the camera templates and anatomic markers is used on each imaging day. Later calculations are simplified by acquiring all patient images for 300 sec. The ^{131}I camera standard is imaged for one minute at a fixed distance of 30 cm during each session.

Every time the patient is imaged, a whole-body radioiodine retention determination is also performed. The patient radioiodine content is measured by having the patient stand five meters from a heavily shielded uptake probe while counts are accumulated for one minute each, both anteriorly and posteriorly. The standard is also counted for one minute at a fixed distance. One minute background counts are acquired. Net patient whole-body uptake is determined by background subtracted geometric mean of the anterior and posterior counts decay corrected by comparison to the standard counts.

IMAGE ANALYSIS

A rectangular region of interest drawn around the imaging standard flask supplies total counts for calculation of the system calibration factor (cpm/μCi). Organ regions of interest (ROI) drawn using the ^{99m}Tc images are applied to the ^{131}I antibody images from each timepoint (Fig. 3). Counts in an organ ROI in the anterior and posterior views for each timepoint are generated. Similarly, these same regions are used to derive patient attenuation values from the transmission and field flood images. An understanding of this part of the method is critical. Images of the radioiodinated antibody will lack the resolution and high count rates associated with technetium images. Also, when biodistribution is favorable for treatment, normal organs will not accumulate an appreciable amount of labeled antibody, especially at the later

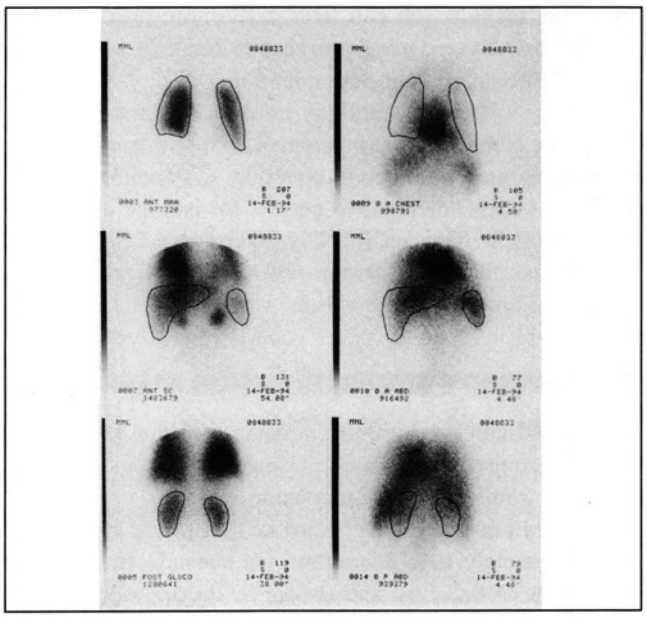

FIGURE 3. Images taken using ^{99m}Tc compounds, left, and ^{131}I-labeled monoclonal antibodies, right. The technetium images are used to draw the regions around the plainly visible organs, and those regions are placed over the iodine images for data retrieval.

imaging timepoints. For these reasons, accurate ROIs cannot be drawn using the images of the trace-labeled antibody. Precisely repositioning the patient on each subsequent day permits the regions drawn using the technetium images to be used for deriving organ radioiodine content at each timepoint. Attention to detail at this phase of the study allows the high degree of reliability and reproducibility necessary to confidently proceed with therapy. Radioiodine organ content and percent injected dose are calculated using Equations 1 and 2.

To maintain consistency and reproducibility throughout our study, we customized a Macintosh-based spreadsheet program to minimize operator interaction after the ROIs are applied to the images. The patient name, number, the date and time of infusion, the microcuries of isotope, amount and type of antibody, the dates and times that images were acquired, and the counts from the various regions are entered by the technologist. All calculations are performed by the spreadsheet program and calculation cells are locked to reduce operator error. Output includes a copy of the data input sheet, calculation sheets, and a summary sheet which lists percent of injected dose in each organ at each timepoint and a graph of the time-activity curves of selected organs.

RESULTS

Since initiation of this method of data acquisition, processing and reporting, we have reduced data processing time by half. This time savings becomes important when a patient qualifies for treatment. It allows us to optimize our schedule for ordering the isotope for therapy; we can treat patients before they develop human antimouse antibody; and patients that require rapid intervention can receive treatment sooner. The time spent acquiring images of organs localized with technetium-labeled products is offset by being able to quickly and confidently position patients after antibody infusion. Processing time was reduced considerably since ROI drawing was done only once, and regions are not moved after being drawn. With this method we are making more efficient use of our time while generating accurate, reproducible data. Consequently, our investigators have a high level of confidence in our results.

DISCUSSION

Accurate data collection and processing are essential to create valid dosimetry estimates for radioimmunotherapy. The method we describe presents a systematic approach. A direct measurement is made of organ-specific patient body attenuation for ^{131}I, which eliminates the need for mathematical approximation of this value. Reproducible, exact patient positioning at each imaging timepoint is achieved, permitting ROI drawing and application that is consistent from image to image and study to study. This method produces total-body disappearance, urine excretion and blood concentration data, and accurate and reliable estimates of radioisotope content in organs. This input data for MIRD calculations of radiation-absorbed dose estimates for normal organs and tumor sites gives information that is consistent and specific for each patient, antibody and dose evaluated. By customizing a personal computer spreadsheet program, data calculation and reporting of the study were streamlined and computational errors were eliminated.

Our procedure is straightforward, can be set up easily and performed by any experienced nuclear medicine technologist. This method gives the investigator a high level of confidence in the absorbed dose estimates to normal organs and tumor from a trace-labeled antibody biodistribution study, and allows observation of true antibody behavior, critical to development of imaging and treatment protocols. Because our study calls for high ^{131}I-labeled antibody doses to be administered for treatment, we must be able to correlate reliably estimated absorbed dose to normal organ toxicity with clinical response. This method of collecting biodistribution data facilitates this important goal in radioimmunotherapy.

ACKNOWLEDGMENTS

The authors wish to thank Holly Pike for her excellent clerical support. This work was supported by Public Health Services grants CA-47430 and 5PO1-CA-44991.

REFERENCES

1. Abrams PG, Carrasquillo JA, Schroff RA et al. Imaging and therapy of metastatic carcinoma with radiolabeled antibodies. In: Oldham RK, ed. *Principles of cancer biotherapy.* New York, NY: Raven Press; 1987:337–354.
2. Carrasquillo JA, Krohn KA, Beaumier P et al. Diagnosis of and therapy for solid tumors with radiolabeled antibodies and immune fragments. *Cancer Treat Rep* 1984;68:317–328.

3. Epenetos AA, Shepherd J, Britton KE et al. ^{123}I radioiodinated antibody imaging of occult ovarian cancer. *Cancer* 1985;55:984–987.
4. Carrasquillo JA, Sugarbaker P, Colcher D et al. Radioimmunoscintigraphy of colon cancer with iodine-I-131-labeled B72.3 monoclonal antibody. *J Nucl Med* 1988;29:1022–30.
5. Eary JF, Schroff RW, Abrams PG et al. Successful imaging of malignant melanoma with Tc-99m-labeled monoclonal antibodies. *J Nucl Med* 1989; 30:25–32.
6. Epenetos AA, Courtenay-Luck N, Pickering D et al. Antibody guided irradiation of brain glioma by arterial infusion of radioactive monoclonal antibody against epidermal growth factor receptor and blood group A antigen. *Br Med J* 1985;290:1463–1466.
7. Larson SM, Carrasquillo JA, Reynolds JC. Radioimmunodetection and radioimmunotherapy. *Cancer Invest* 1984;2:363–381.
8. Nelp WB, Eary JF, Jones RF et al. Preliminary studies of monoclonal antibody lymphoscintigraphy in malignant melanoma. *J Nucl Med* 1987; 28:34–41.
9. Rosen S, Zimmer A, Goldman-Leiken R et al. Radioimmunodetection and radioimmunotherapy of cutaneous T-cell lymphomas using an I-131-labeled monoclonal antibody: an Illinois Cancer Council Study. *J Clin Oncol* 1987;5:562–573.
10. Appelbaum F, Badger C, Eary J, Matthews D, Press O, Bernstein M. Therapy of hematologic malignancies using radioimmunotherapy (RAIT). *Cambridge medical reviews: haematology oncology* 1991;2.
11. Bernstein ID, Eary JF, Badger CC et al. High dose radiolabeled antibody therapy of lymphoma. *Cancer Res* 1990;50(Suppl.):1017s–1021s.
12. DeNardo S, DeNardo G, O'Grady L et al. Pilot studies of radioimmunotherapy of B-cell lymphoma and leukemia using I-131 Lym-1 monoclonal antibody. *Antibody, Immunoconj, Radiopharm* 1988;1:17–23.
13. Eary JF, Press OW, Badger CC et al. Imaging and treatment of B-cell lymphoma. *J Nucl Med* 1990;31:1257–1268.
14. Eary JF. Radioimmunotherapy of B-cell lymphoma. *Ann Oncol* 1991; 2(Suppl):187–190.
15. Ferens JM, Krohn KA, Beaumier PL et al. High-level iodination of monoclonal antibody fragments for radiotherapy. *J Nucl Med* 1984;25: 367–370.
16. Horowitz JA, Goldenberg DM, DeJager R et al. Phase I/II trial of radioimmunotherapy (RAIT) with I-131-labeled anti-CEA and anti-AFP monoclonal antibodies (Mabs) [abstract.] *J Nucl Med* 1988;29:846.
17. Kalnicki S, Bloomer W. Antibody radiotherapy: current status. In: M. Z. Zalutsky, eds. *Antibodies in radiodiagnosis and therapy.* Boca Raton, FL: CRC Press, Inc., 1989:199–211.
18. Order S, Stilwagon G, Klees J et al. Iodine 131 antiferritin, a new treatment modality in hepatoma; a radiation therapy oncology group study. *J Clin Oncol* 1985;3:1573–1582.
19. Press OW, Eary JF, Badger CC et al. Treatment of refractory non-Hodgkin's lymphoma with radiolabeled MB-1 (anti-CD37) antibody. *J Clin Oncol* 1989;7:1027–1038.
20. Press OW, Eary JF, Badger CC et al. High dose radioimmunotherapy of B cell lymphomas with autologous marrow rescue. In: J. Vaeth, ed. *Frontiers in radiation therapy and oncology.* Basil, Switzerland: Kargar AG, 1989:204–213.
21. Press OW, Appelbaum F, Ledbetter JA et al. Monoclonal antibody 1F5 (anti-CD20) serotherapy of human B cell lymphomas. *Blood* 1987;69:584–591.
22. Greenwood FC, Hunter WM, Glover J. The preparation of I-131 labeled human growth hormone by high specific activity radioactivity. *Biochem J* 1963;89:114–123.
23. Eary JF, Appelbaum FL, Durack L et al. Preliminary validation of the opposing view method for quantitative gamma camera imaging. *Med Phys* 1989;16:382–387.
24. Bice AN, Eary JF, Nelp WB. Quantification of Iodine-131 distribution by gamma camera imaging (letter). *Eur J Nucl Med* 1991;18:142–144.
25. Eary JF. Correlative imaging in radioimmunotherapy. *Invest Radiol* 1991; 26:755–760.
26. Hammond ND, Moldofsky PJ, Beardsley MR et al. External imaging techniques for quantitation of distribution of I-131 F(ab')2 fragment of monoclonal antibody in humans. *Med Phys* 1984;11:778–783.
27. Thomas SR, Maxon HR, Kerelakes JG et al. Quantitative external counting techniques enabling improved diagnostic and therapeutic decisions in patients with well-differentiated thyroid cancer. *Radiology* 1977;122:731–737.
28. Cloutier RJ, Watson EE, Rohrer RH et al. Calculating the radiation dose to an organ. *J Nucl Med* 1973;14:53–55.
29. Snyder W, Ford M, Warner G. Estimates of specific absorbed fractions for photon sources uniformly distributed in various organs of a heterogeneous phantom. *MIRD Pamphlet #5.* New York, NY: Society of Nuclear Medicine; 1978.
30. Loevinger R, Budinger T, Watson E. *MIRD primer for absorbed dose calculations.* New York, NY: Society of Nuclear Medicine; 1988.
31. Heymsfield SB, Fulenwider T, Nordlinger B et al. Accurate measurement of liver, kidney and spleen volume and mass by computerized axial tomography. *Ann Intern Med* 1979;90:185–187.